Structural studies of nanosized porous membrane catalytic systems highly active in dry reforming of biomass conversion products*

M. V. Tsodikov,[a] V. V. Teplyakov,[a] A. S. Fedotov,[a] V. I. Uvarov,[b] D. Roizard,[c] A. Kiennemann,[d] C. Courson,[d] and I. I. Moiseev[a]*

[a]*A. V. Topchiev Institute of Petrochemical Synthesis, Russian Academy of Sciences, 29 Leninsky prosp., 119991 Moscow, Russian Federation. Fax: +7 (495) 633 8520. E-mail: tsodikov@ips.ac.ru*
[b]*Institute of Structural Macrokinetics and Materials Science, Russian Academy of Sciences, 142432 Chernogolovka, Moscow Region, Russian Federation. Fax: +7 (496) 524 6222*
[c]*Laboratory of Reactions and Technologies of Processes, Higher National School of Chemical Industry, Lorraine National Polytechnic Institute, 1 rue Grandville, BP 20451, 54001 Nancy CEDEX, France.** Fax: +33 (03) 83 35 08 11*
[d]*Laboratory of Materials, Surfaces, and Catalytic Processes, European School of Chemistry, Polymers, and Materials, Strasbourg University, 25 rue Becquerel, 67087 Strasbourg CEDEX 2, France.*** Fax: +33 (03) 68 85 26 74*

The structures of porous ceramic membrane catalytic systems exhibiting high activity in dry reforming of biomass conversion products (methane, hydrocarbons C_2—C_4, and alcohols) to a hydrogen-containing gas were studied. The membrane catalytic systems represent porous inorganic membranes (supports) prepared by self-propagating high-temperature synthesis and modified by nanosized metallocompex components, which are uniformly distributed in the internal pore volume. Structural studies were carried out using scanning electron microscopy with energy dispersive analysis, transmission electron microscopy, temperature-programmed reduction with hydrogen, and X-ray diffraction analysis.

Key words: membrane catalytic systems, porous inorganic membranes, microreactor, nanocatalyst, dry reforming, biomass, structure.

Considerable attention is recently given to the development of efficient methods for the conversion of natural gas and renewable biomass to syn-gas and dihydrogen, which are among the major energy carriers in petroleum chemistry and power engineering.[1—3] It has previously been shown that the dry reforming and vapor reforming of methane, its gaseous homologies, alcohols, and a series of carboxylic acids (primary products of biomass conversion) are substantialy intensified in porous membrane catalytic systems (MCS). These systems have a very low content of active components distributed on the internal surface of the membrane channels.[4—6] However, they exhibit high specific productivity in the formation of syngas in dry reforming of methane and ethanol. Syn-gas production increases if a mixture of ethanol and glycerol (50%) mixture is used as raw materials.[7] The productivity of syn-gas for the process in the membrane catalytic reactor increases by almost an order of magnitude compared to that attained when dry reforming is carried out in a traditional flow-type reactor with the loaded stationary catalyst bed of a similar composition obtained by grinding the MCS.[4—7]

As shown in many works, the improved heat exchange and mass transfer of the substrates in membrane channels are important advantages of such systems compared to the stationary catalyst bed loaded in a traditional flow-type reactor.[8,9]

* Dedicated to Academician of the Russian Academy of Sciences R. Z. Sagdeev on the occasion of his 70th birthday.

** Laboratoire Réactions et Génie des Procédés de l´Ecole Nationale Supérieure des Industries Chimiques de l´Institut National Polytechnique de Lorraine, 1 rue Grandville, BP 20451, 54001 Nancy CEDEX, France.

France, 1 rue Grandville, BP 20451, 54001 Nancy CEDEX.

*** Laboratoire des Matériaux, Surfaces et Procédés pour la Catalyse de l´Ecole Européenne de Chimie, Polymères et Matériaux de l´Université de Strasbourg, France, 25 rue Becquerel, 67087 Strasbourg CEDEX 2.

Published in Russian in *Izvestiya Akademii Nauk. Seriya Khimicheskaya,* No. 12, pp. 2537—2545, December, 2011.

1066-5285/11/6012-2588

To get insight into the features of conversion of organic substrates in catalytic microchannels of the membranes, it is important to know the macrokinetic parameters and also the structure, the main physicochemical characteristics, and the charge states and phase transitions of active components during both MCS preparation and catalysis.

In this work, we studied the structure, porosity, and genesis of the bimetallic active components distributed on the surface of the porous membranes obtained by self-propagating high-temperature synthesis (SPHTS).

Experimental

The MCS containing active components La—Ce, Pd—Co, and Pd—Mn, which exhibited the highest activity and selectivity in dry reforming and vapor reforming of methane, light hydrocarbons, alcohols, and acetic acid (primary products of biomass conversion) are the objects of the study.[4—7]

The MCS samples represent thermally stable (>1000 °C) porous (porosity ~40%) ceramic membrane supports with the finger configuration and 130 mm in length with an external diameter of 15 mm and a wall thickness of 4 mm (Fig. 1) prepared from highly dispersed powders Ni(86.4%)—Al(13.6%) by the SPHTS method[10] and modified by the presence of the metal oxide catalysts.[11]

The catalytic layer of the active components was formed in the internal volume of the membrane channels by the alkoxo method on the basis of organic solutions of the metallocomplex precursors containing La—Ce, Pd—Co, and Pd—Mn.[12,13]

The ratio of components of the La—Ce-containing catalytic system was chosen on the basis of the literature data on dry reforming of methane in the traditional reactor with the bulk bed of the La—Ce/MgO catalyst, which manifested the highest activity in dry reforming of methane.[14]

To form catalytic coatings on the internal surface of the membrane channels, mother liquors of metallocomplex precursors in toluene was pumped through the membrane on the laboratory setup connected to a vacuum pump. Then wet heated air was blown through the membrane, and the membrane was dried *in vacuo* (1 Torr) and subjected to the high-temperature treatment at 300, 500, and 700 °C (Fig. 2).

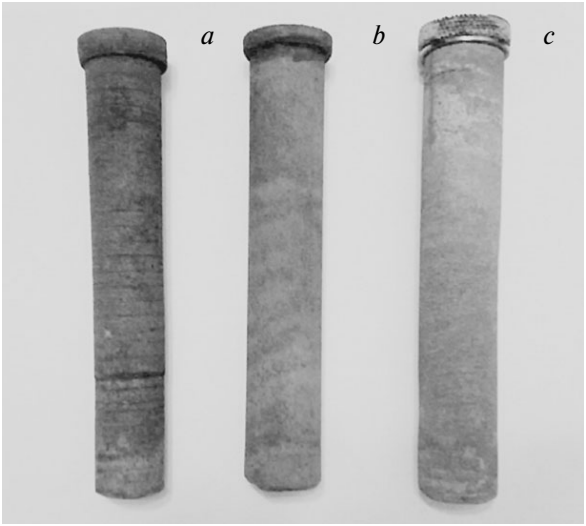

Fig. 1. Samples of ceramic membranes of different composition containing Co (*a*), Ni (*b*), and Fe (*c*).

Prior to the formation of the coating of the catalytically active components, a buffer layer of titania was deposited on the internal walls of the membrane channels to increase the specific surface area and to decrease the pore size. For this purpose, a colloidal mother liquor of titanium *n*-butoxide stabilized by acetylacetonate was pumped through the membrane microchannels.

The amount of supported titania was monitored by an increase in the membrane weight after deposition of titania and thermal treatment. The supporting procedure was repeated 4—6 times until a coating containing 3.2—3.5 wt.% titania with respect to the initial membrane weight was formed. Once the buffer layer of titania was deposited, the metal oxide catalytic coating was formed on the internal surface of the microchannels.

The [La—Ce]—MgO catalytic system was formed by the consecutive deposition of magnesium acetylacetonate stabilized by monoethanolamine in a toluene solution. After the thermal treatment of the magnesium-containing coating, a mother liquor of the acetylacetone-chelated lanthanum and cerium complexes in methanol was deposited on the internal surface of the membrane. Then the membrane was dried in a draft hood in a flow of wet heated air, evacuated at 80 °C (45 min), and subjected to thermal treatment in a muffle furnace to remove organic moieties at 500 (30 min), 600 (30 min), and 700 °C (4 h).

Titanium *n*-butoxide in combination with Pd—$M(OAc)_4 \cdot \cdot H_2O$ homo- and heterometallic acetate complexes, prepared according to a procedure described above,[12,13] was used to form the Pd—M-containing catalytic system (M = Co or Mn) in the internal volume of the ceramic membrane.

A colloidal solution containing precursors of the Pd—M catalytic system was prepared as follows: titanium *n*-butoxide in an argon flow was diluted with absolute toluene in a volume ratio of 1 : 1 and stabilized by acetylacetone added in an equimolar amount. The obtained mixture was magnetically stirred for 30 min at ~20 °C.

The acetate complexes in amounts needed to form the Pd—M/TiO_2 oxide systems containing 2% Pd and 1% M with respect to TiO_2 (Table 1) were dissolved in methanol at ~20 °C. The obtained 2% solutions of bimetallic Pd-containing acetate complexes in methanol were added with stirring in argon to a stabilized solution of titanium butoxide. The reaction mixture was magnetically stirred for 30 min in argon. The mother liquors of the Pd—Co- and Pd—Mn-containing components were thus prepared and pumped through the pores modified by the buffer titania coating. After deposition of the mother liquor containing

Table 1. Content (*m* (wt.%)) of the first (m_1) and second (m_2) component in the MCS

m_1	m_2	m_1/m_2
La	Ce	0.020/0.035
Pd	Co	0.014/0.007
Pd	Mn	0.015/0.008

* The weight of the membrane is ~100 g.

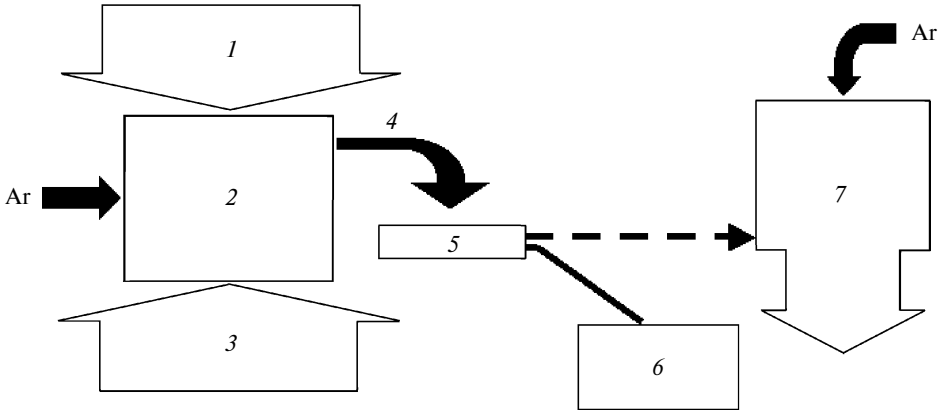

Fig. 2. Sequence of modification of the internal surface of the membrane channels with the catalytic coating: (*1*) precursors, (*2*) organic colloidal solution, (*3*) solvent and sol stabilizers, (*4*) mother liquor→gel, (*5*) membrane, (*6*) vacuum pump, and (*7*) muffle furnace (≤500—700 °C).

the complexes of the active components, the MCS were subjected to thermal treatment in the regime similar to that described above for the La—Ce-containing system.

The content of the supported metal-containing active components determined by laser microanalysis and atomic absorption spectroscopy is given in Table 1.

The structure and composition of the MCS was studied by scanning electron microscopy with energy dispersion X-ray analysis (SEM-EDA), transmission electron microscopy (TEM), X-ray diffractometry (XRD), temperature-programmed reduction with hydrogen (TPR), low-temperature nitrogen adsorption (BET), and mercury porometry.

A JEOL JSM-6700F scanning electron microscope with an energy dispersion X-ray analyzer was used. An autoemission cobalt cathode (^{57}Co, A = 50 mCi) served as an emitter. Since the studied systems have electron conductivity *per se*, they were analyzed without special pre-experimental procedures.

The fine structure of the catalytic membrane materials was studied by the TEM method on a TOPCON EM-002B superhigh-resolution transmission electron microscope using a hexaboride—lanthanum filament (LaB_6, U_{max} = 200 kV). Small sections obtained by cutting the membrane with a diamond saw to prevent destruction of the sample surface were used in this analysis.

The phase composition of the samples was studied on a Bruker AXS D8 Advance X-ray diffraction setup equipped with a Vantec detector with a graphite monochromator and a high-intensity copper anticathode (Cu-Kα radiation, λ = 1.54 Å). A focusing Johansson-type monochromator was mounted on the diffractometer, which made it possible to obtain high-intensity radiation in a narrow range of the $K\alpha_1$ line and to analyze sample in both reflection and transmission modes. The crystalline phases were identified on the basis of the DIFFRAC^{plus} EVA database.

Reducibility of the oxide phase of the catalytically active components of the MCS was studied by TPR. For this purpose, a weighed sample (100 mg) was heated in a hydrogen flow with a rate of 15 °C min^{-1} in the temperature range from 25 to 900 °C. Then, using the calibration tables and reference data, the oxide phases of metals were identified from the characteristic peaks and their relative content on the surface was calculated.

The specific surface was studied by low-temperature nitrogen adsorption on Thermo Scientific Sorptomatic 1990 and Micromeritics TriStar 3000 instruments using dinitrogen as a sorbed gas. The calculations were performed by the BET method using desorption and adsorption isotherms.

The pore sizes and their distribution over the sample surface were determined by mercury porometry according to the model of cylindrical pores on a Micromeritics AutoPore IV precision mercury porometer.

Results and Discussion

The data of mercury porometry and low-temperature nitrogen adsorption are given in Table 2. It is seen that the buffer layer formed in the membrane pores substantially decreases the effective pore diameter and, hence, increases the specific surface. The effective pore diameter and

Table 2. Structural parameters of the MCS

Sample, MCS	d*/nm	Porosity (%)	Channel length/mm	S_{sp}/m^2 g^{-1}
Ni—Al membrane support	224.9	38.0	0.3	0.08
[La—Ce]—MgO—TiO_2/Ni—Al	48.8	20.2	0.2	0.30
[Pd—Mn]—TiO_2/Ni—Al	88.0	12.9	0.2	0.16
[Pd—Co]—TiO_2/Ni—Al	58.8	16.2	0.3	0.35

* Average pore diameter.

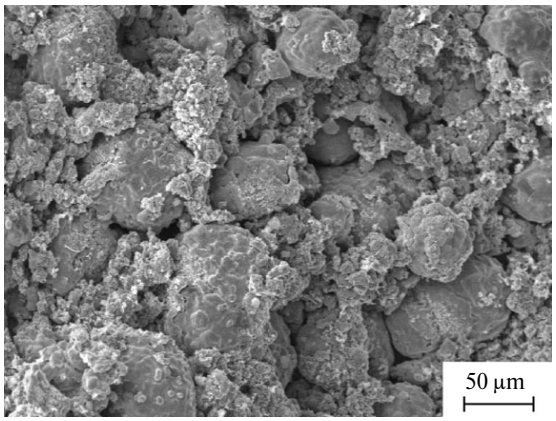

Fig. 3. Image of the cross section of a sample of the porous ceramic membrane.

porosity decrease ~2—4 times (see Table 2), which can be due to "loosening effect" of the structure of the supported oxide obtained by the alkoxo method from colloidal solutions. The same change in the pore parameters has been observed previously[15] for the metalloceramic membranes (Trumem trade mark). The catalytic layer of the complex oxide $Cu_xTi_{1-0.5x}O_{2\pm\delta}$ was formed using the alkoxo method on the internal surface of the Trumem membranes. It was found[15] that the ceramic membranes have comparatively high (for metals) specific surface, which also increases 2—4 times when coated with a small amount of the catalyst. After this procedure, the average channel length remains almost unchanged, which indicates, most likely, an increase in pore tortuosity.

The morphology and elemental composition of the MCS were studied by the SEM-EDA method. The cross section of the sample of the unmodified Ni—Al membrane is shown in Fig. 3. As can be seen, its porous structure is formed by fine granules of Al and larger granules of Ni.

As follows from the SEM-EDA images for the modified MCS, the supported catalytic components are uniformly distributed over the surface of the studied samples. Structural oxygen was found, which is also uniformly distributed, indicating that these components exist as oxides (Figs 4 and 5). The presence of oxygen in a fairly high concentration on the MCS surface confirms the thermogravimetric analysis results for the behavior of the catalyst during dry reforming of methane and ethanol.[4,5] It was shown[4,5] that the first step of organic substrate conversion in dry reforming is their partial and deep oxidation by surface oxygen, resulting in a decrease in the catalyst weight and formation of the CO, CO_2, and water vapors in the gas phase.

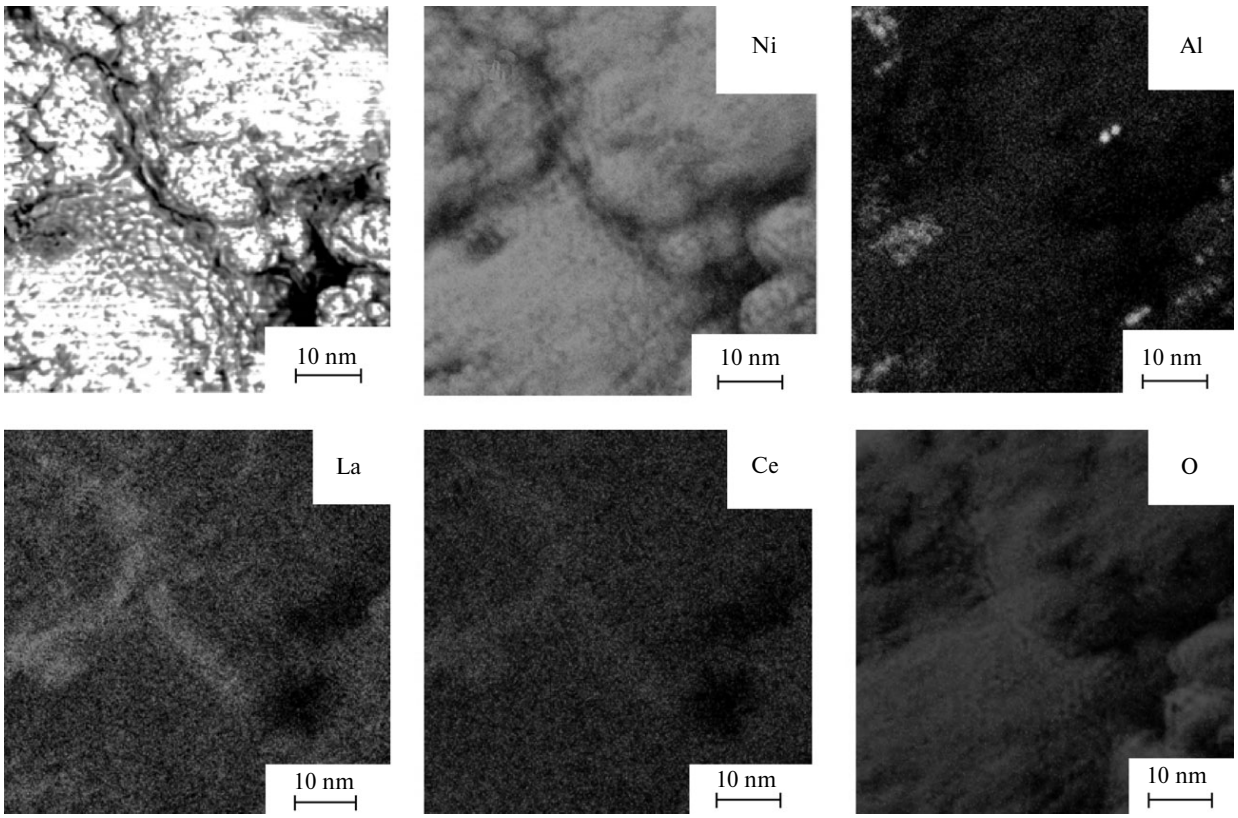

Fig. 4. Distribution of elements over the MCS surface of the composition [La—Ce]—MgO—TiO_2/Ni—Al.

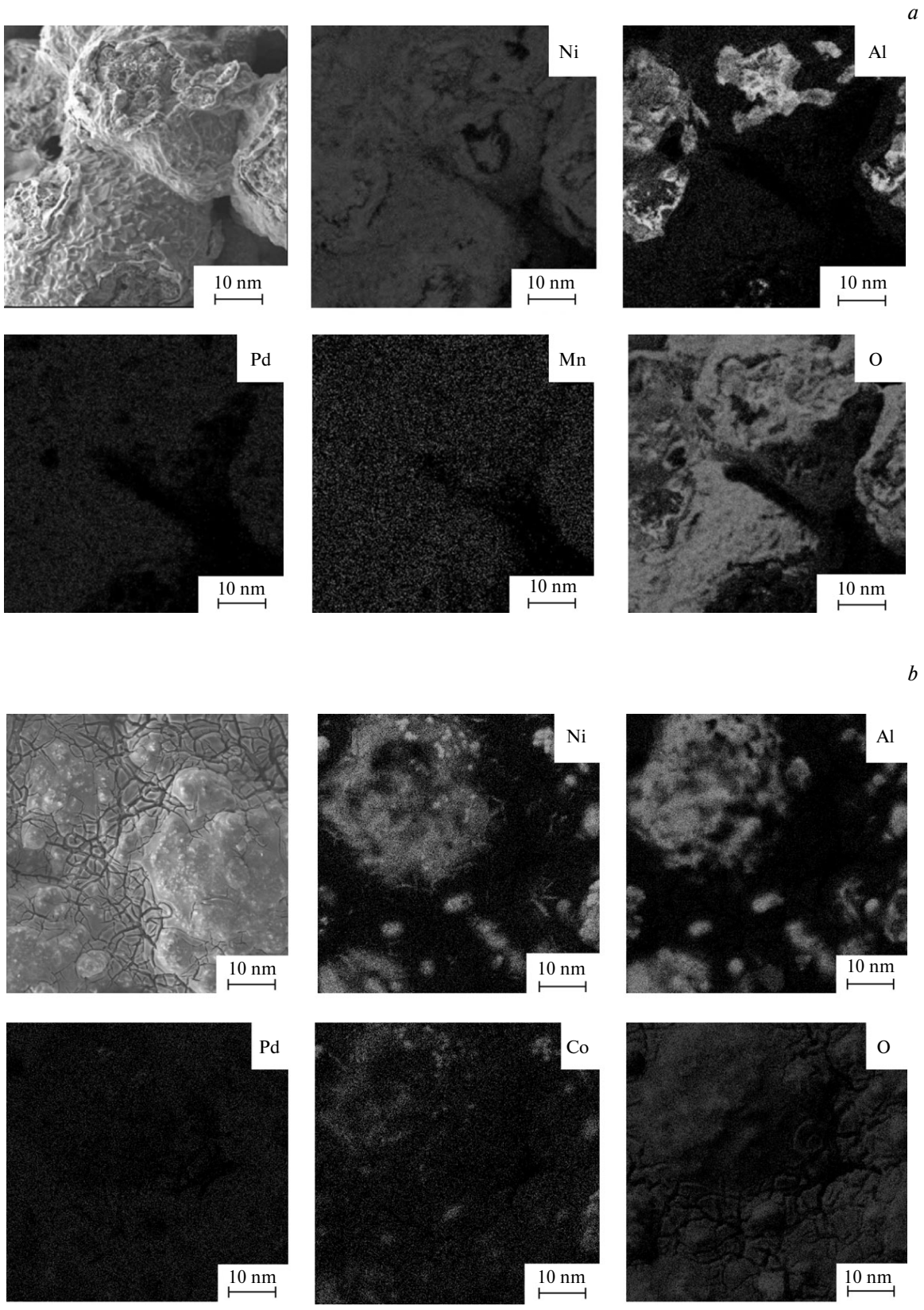

Fig. 5. Distribution of elements over the MCS surface of different compositions: [Pd—Mn]—TiO_2/Ni—Al (*a*) and [Pd—Co]—TiO_2/Ni—Al (*b*).

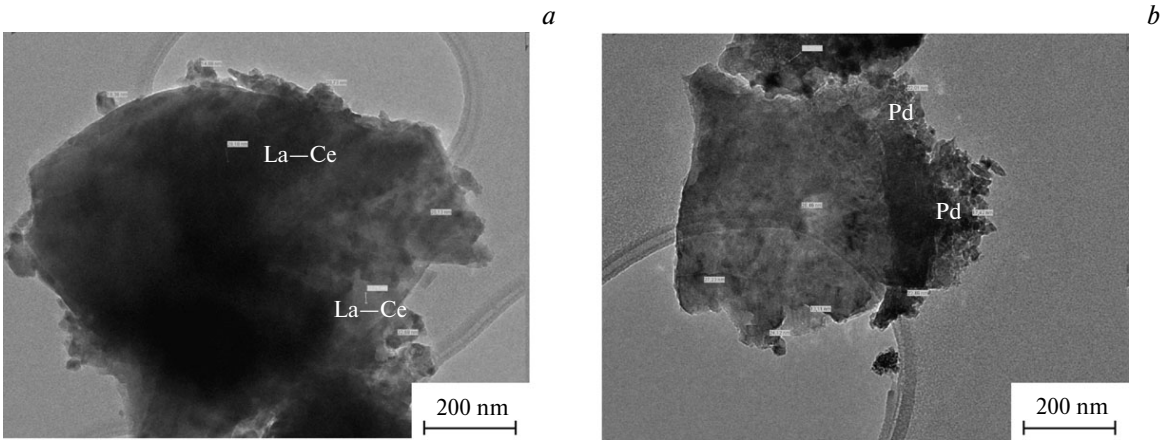

Fig. 6. Clusters of the supported La—Ce- (*a*) and Pd-containing catalysts (*b*) on the Ni—Al membrane surface (sites of performing elemental analysis are marked).

$$CH_4 + 0.5\ O_2 \rightarrow CO + 2\ H_2, \quad (1)$$

$$CH_4 + 2\ O_2 \rightarrow CO_2 + 2\ H_2O. \quad (2)$$

The TEM study of the fine structure of the material of the membrane catalytic systems showed that the averaged cluster size in the supported catalysts is approximately the same and equals 15—20 nm (Fig. 6).

Thus, the formation of a porous buffer coating of porous TiO_2 makes it possible to uniformly distribute metal-containing active components with a similar size. The alkoxo method used for the solution of this problem seems very promising.

Since the studied systems exhibit high activity in dry, vapor, and mixed dry—vapor reformings of hydrocarbons and alcohols with the formation of hydrogen-containing gas, we studied possible transformations of the active components in the presence of dihydrogen by the TPR method.

The TPR curve of the initial Ni—Al membrane is shown in Fig. 7. As can be seen, the initial membrane Ni—Al support remains nearly unreduced in the whole temperature range studied, which indicates a very insignificant concentration of oxides on the surface.

The TPR results for the [La—Ce]—MgO—TiO_2/Ni—Al MCS are shown in Fig. 8.

The TPR curve for the La—Ce-containing system contains three peaks. The first peak at 450 °C, according to the literature data, corresponds to the reduction of nickel oxide and the transition of $Ni^{2+}O$ to Ni^0 by reaction (3). The second and third peaks in the temperature range from 700 to 900 °C are related to the reduction of cerium oxide (Ce^{4+} to Ce^{3+}) by reaction (4).[16]

$$Ni^{2+}O + H_2 \rightarrow Ni^0 + H_2O \quad (3)$$

$$2\ Ce^{4+}O_2 + H_2 \rightarrow Ce^{3+}{}_2O_3 + H_2O \quad (4)$$

The calculation of the relative content of the oxide phases of metals on the surface of the studied sample

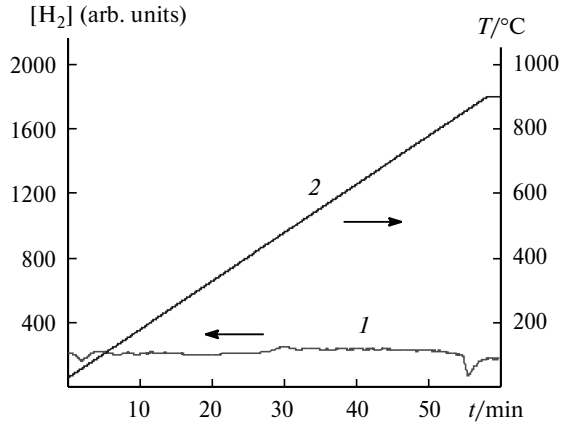

Fig. 7. Temperature-programmed reduction of the Ni—Al membrane support: *1*, TPR curve and *2*, temperature *vs* time.

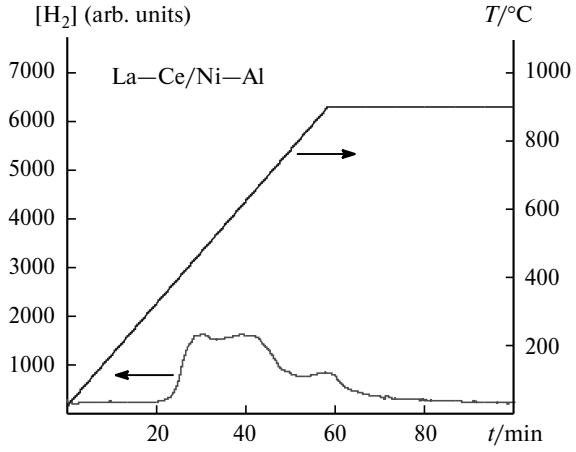

Fig. 8. Temperature-programmed reduction of the [La—Ce]—MgO—TiO_2/Ni—Al MCS: *1*, TPR curve and *2*, temperature *vs* time.

showed that $1.34 \cdot 10^{-4}$ mole of oxides was reduced in the TPR process, of which the fraction of $Ni^{2+}O$ was $\sim 0.47 \cdot 10^{-4}$ mol (35%) and that of $Ce^{4+}O_2$ was $\sim 0.87 \cdot 10^{-4}$ mol (65%).

The oxide phases of the [Pd—Mn]—TiO_2/Ni—Al MCS are reduced in the temperature range 350—650 °C, which can be attributed to the reduction of nickel and palladium oxides ($Ni^{2+}O \rightarrow Ni^0$, $Pd^{2+}O \rightarrow Pd^0$).[17] According to the literature data, the peak appeared in the temperature range 750—900 °C is caused, most likely, by the reduction of manganese oxide ($Mn^{3+}{}_2O_3 \rightarrow Mn^{2+}O$)[18] (Fig. 9).

The thermoreduction of the considered oxide proceeds according to reactions (3), (5), and (6).

$$Pd^{2+}O + H_2 \rightarrow Pd^0 + H_2O \quad (5)$$

$$Mn^{3+}{}_2O_3 + H_2 \rightarrow 2\ Mn^{2+}O + H_2O \quad (6)$$

Thus, $6.58 \cdot 10^{-5}$ mole of the oxide phases of the surface was reduced during the experiment, $\sim 3.98 \cdot 10^{-3}$ mol (78%) of which is accounted for by $Ni^{2+}O$ and $Pd^{2+}O$, whereas $Mn^{3+}{}_2O_3$ gives $\sim 1.44 \cdot 10^{-5}$ mol (22%).

Four peaks are observed in the curve of reduction of the [Pd—Co]—TiO_2/Ni—Al MCS (Fig. 10).

The first peak at 450 °C is attributed to the reduction of nickel(II) oxide *via* reaction (3). Two subsequent peaks in the range from 500 to 700 °C corresponds to the reduction of palladium(II) oxide *via* reaction (5) and cobalt oxide with the mixed valence Co_3O_4 ($Co^{II}O \cdot Co^{III}{}_2O_3$). According to the published data,[19] the latter proceeds in two steps.

$$Co^{2+,3+}{}_3O_4 + H_2 \rightarrow 3\ Co^{2+}O + H_2O \quad (7)$$

$$Co^{2+}O + H_2 \rightarrow Co^0 + H_2O \quad (8)$$

The fourth peak at 900 °C is associated, probably, with the thermal decomposition of unreduced mixed cobalt oxide ($CoO \cdot Co_2O_3$)[20] followed by the interaction of

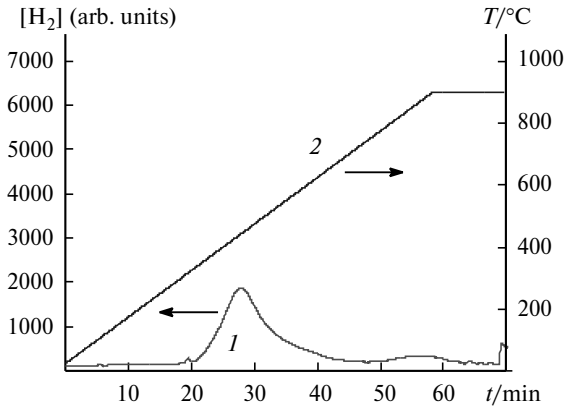

Fig. 9. Temperature-programmed reduction of the [Pd—Mn]—TiO_2/Ni—Al MCS: *1*, TPR curve and *2*, temperature *vs* time.

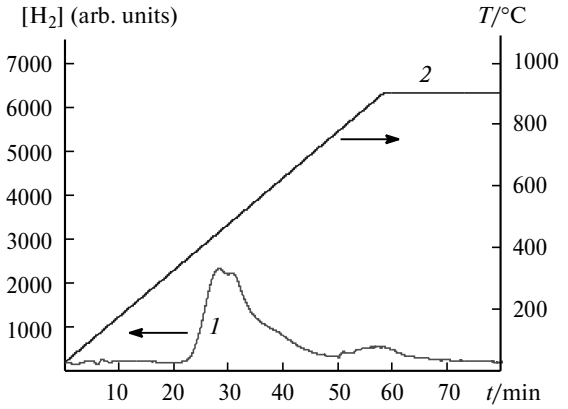

Fig. 10. Temperature-programmed reduction of the [Pd—Co]—TiO_2/Ni—Al MCS: *1*, TPR curve and *2*, temperature *vs* time.

evolved dioxygen with dihydrogen and the formation of water *via* reactions (9) and (10).

$$2\ Co^{2+,3+}{}_3O_4 \rightarrow 6\ Co^{2+}O + O_2 \quad (9)$$

$$2\ H_2 + O_2 \rightarrow 2\ H_2O \quad (10)$$

Cobalt(II) oxide formed in reaction (9) is additionally reduced to the metallic state according to reaction (8).[19]

The quantitative analysis of the content of the oxide phases on the surface of the studied sample showed that $\sim 0.9 \cdot 10^{-4}$ mole of oxides was reduced in the experiment. The metal oxides presented are reduced in rather close temperature ranges and in many steps, as in the case of complex cobalt oxide. Therefore, it is important to evaluate the content of particular oxides of this MCS even approximately.

According to the XRD results, the membrane materials mainly consists of cubic $AlNi_3$ and nickel metal. The presence of nickel carbide (NiC) and free carbon also cannot be excluded (Fig. 11).

Nickel is present predominantly as cubic NiO in the structures of the [La—Ce]—MgO—TiO_2/Ni—Al, [Pd—Mn]—TiO_2/Ni—Al, and [Pd—Co]—TiO_2/Ni—Al

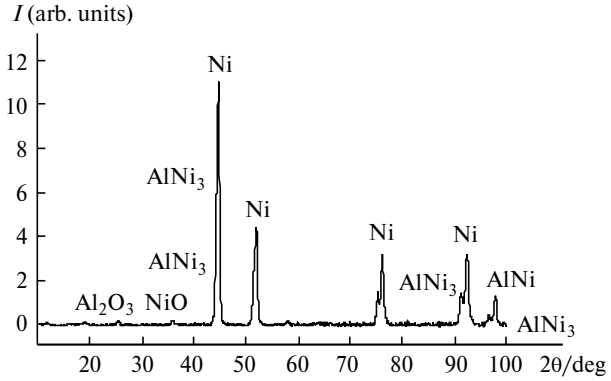

Fig. 11. XRD pattern of the Ni—Al membrane support.

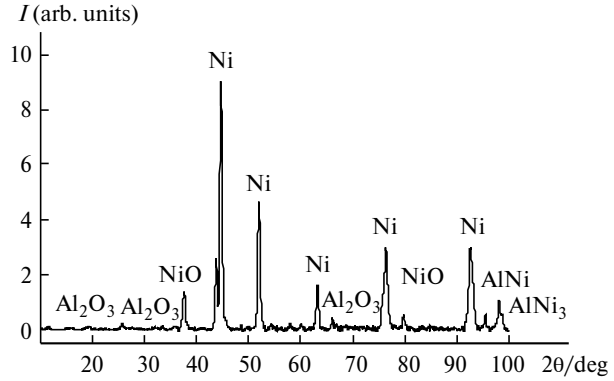

Fig. 12. XRD pattern of the [La—Ce]—MgO—TiO_2/Ni—Al, [Pd—Mn]—TiO_2/Ni—Al, and [Pd—Co]—TiO_2/Ni—Al MCS.

MCS (Fig. 12). The diffractogram is only slightly different from the shapes of the diffraction patterns for the three samples of MCS, which reflects the phase composition of the membrane support. We failed to observe the nanosized phases of the metal oxide catalytic components by XRD, which were identified by SEM-EDA and TEM. Evidently, their content is very low and the dispersity of the phases is too high to be identified by XRD.

As follows from the results of the structural studies, the initial membrane contains almost no phase due to nickel oxide. The TPR and XRD data indicate that the formation of the nickel oxide phase is preceded by the formation of the highly dispersed oxide phase. The NiO phase is formed, most probably, due to solid-phase transformations between the supported metal oxides and initial membrane surface at the step of thermal treatment of the MCS during the preparation of the metal oxide catalysts.

The formation of highly dispersed phases of metal oxides noticeably changes the pore structure of the MCS: the effective pore diameter decreases and their specific surface increases, resulting in pore tortuosity. It has earlier shown for complex oxides $Cu_xTi_{1-0.5x}O_{2\pm\delta}$ formed in pores of the metalloceramic membrane as active components of CO oxidation that the volume of the oxide phase obtained by the alkoxo method and estimated by the permeability data 3—4 times exceeds the volume obtained by the results of determination of the density of the supported material.[15] Therefore, the effective averaged pore size turned out to be substantially smaller than it was expected with allowance for the calculation data.[15]

The ceramic membranes obtained by the SPHTS method contain up to 10^7 pores per 1 cm^2 of the surface with the effective diameter to 3 μm. After their modification with the metal-containing nanosized active components, the open membrane pores can be considered as an "ensemble" of nanoreactors. In the channels of the porous membrane, the fraction of the surface of the nanosized active components is substantially higher than that of the granules of the catalysts loaded in a traditional flow-type reactor. The previous theoretical analysis of gaseous transport in the membrane pores modified by dispersed systems suggested an increased contribution of transversal diffusion of the substrates in the mass transfer.[21] An increased dispersity of the active components along with the restricted volume of the channels in which they are distributed facilitate, most probably, the accessibility of active sites to gaseous molecules of the substrates that provides favorable conditions for the intensification of catalytic reforming processes.

The alkoxo method used in this work represents an efficient method for the formation of hybrid MCS containing nanosized metal oxide catalysts uniformly distributed in the internal volume of microchannels of the porous membrane.

One of the most important trends in the development of catalytic chemistry is breaking up chemical productions into smaller units aimed at improving monitoring and, hence, at increasing the level of ecological safety. In this context, the development of the membrane catalytic module manifesting high activity in reforming of hydrocarbons and the primary biomass conversion products is a promising approach to the construction of small-size mobile installation for the high-performance production of syngas consumed in important petrochemical processes.

This work was financially supported by the Council on Grants at the President of the Russian Federation (Program for State Support of Leading Scientific Schools of the Russian Federation, Grant NSh-10.2010.10), CNRS, the Russian Foundation for Basic Research (Project No. 11-03-00777-a), and the State Contract No. 16.516.11.6141.

References

1. R. A. Sheldon, *Tez. dokl. Mezhdunar. nauch. konf.* [*Abstrs Intern. Scientific Conf.*] *"Europacat IX"* (*Salamanca, Spain, August 30—September 4, 2009*), Salamanca, 2009, 107.
2. R. M. Baldwin, *Tez. dokl. Mezhdunar. nauch. konf.* [*Abstrs Intern. Scientific Conf.*] *"9th Novel Gas Conversion Symposium C_1 — C_4 Chemistry from Fossil to Bio Resources" (Lyons, France, May 30—June 3, 2010)*, Lyons, 2010, 23.
3. S. D. Varfolomeev, I. I. Moiseev, B. F. Myasoedov, *Vestn. Ros. akad. nauk* [*Bulletin of the Russian Academy of Sciences*], 2009, **79**, 595 (in Russian).
4. M. V. Tsodikov, A. S. Fedotov, V. V. Teplyakov, D. Ruazar, V. N. Korchak, V. Yu. Bychkov, V. I. Uvarov, I. I. Moiseev, *Izv. Akad. Nauk*, *Ser. Khim.*, 2011, 54 [*Russ. Chem. Bull.*, *Int. Ed.*, 2011, **60**, 55].
5. M. V. Tsodikov, A. V. Chistyakov, F. A. Yandieva, V. V. Zhmakin, A. E. Gekhman, I. I. Moiseev, *Kataliz v promyshlennosti* [*Catalysis in Industry*], 2010, **5**, 155 (in Russian).
6. A. Fedotov, V. Zhmakin, M. Tsodikov, I. Moiseev, *Tez. dokl. Mezhdunar. nauch. konf.* [*Abstrs Intern. Scientific Conf.*] *"First Workshop of COST Action CM0903 "Utilisation of Biomass for Sustainable Fuels and Chemicals* (*UBIOCHEM)"" (Cordoba, Spain, May 13—15, 2010*), Cordoba, 2010, 25.

7. M. V. Tsodikov, A. S. Fedotov, V. V. Zhmakin, K. B. Golubev, V. N. Korchak, V. N. Bychkov, N. Yu. Kozitsyna, I. I. Moiseev, *Membrany i membrannye tekhnologii* [*Membranes and Membrane Technologies*], 2011, **1**, No. 2, 1 (in Russian).
8. A. A. Khasin, *Zh. Ros. Khim. o-va im. D. I. Mendeleeva*, 2003, **47**, 69; 36 [*Mendeleev Chem. J.* (*Engl. Transl.*), 2003, **47**].
9. F. Kapteijn, J. J. Heiszwolf, T. A. Nijhuis (Xander), J. A. Moulijn, *Ind. Catal.*, *DelftChemTech*, 1999, **3**, 24.
10. V. I. Uvarov, I. P. Borovinskaya, A. G. Merzhanov, Pat. RF No. 2175904, B22F3/10, B22F3/23, C22C1/08 — 2001; *Byul. Izobr.* [*Invention Bulletin*], 2001, No. 32 (in Russian).
11. M. V. Tsodikov, V. V. Teplyakov, A. S. Fedotov, O. V. Bukhtenko, T. N. Zhdanova, V. I. Uvarov, I. P. Borovinskaya, I. I. Moiseev, Pat. RF No. 2325219, B0 1D 71-02, CO 1B 3/38, 2008; *Byul. Izobr.* [*Invention Bulletin*], 2008, No. 15 (in Russian).
12. N. Yu. Kozitsyna, S. E. Nefedov, F. M. Dolgushin, N. V. Cherkashina, M. N. Vargaftik, I. I. Moiseev, *Inorg. Chim. Acta*, 2006, **359**, 2072.
13. N. S. Akhmadullina, N. V. Cherkashina, N. Yu. Kozitsyna, I. P. Stolarov, E. V. Perova, A. E. Gekhman, S. E. Nefedov, M. N. Vargaftik, I. I. Moiseev, *Inorg. Chim. Acta*, 2009, **362**, 1943.
14. A. G. Dedov, A. S. Loktev, I. I. Moiseev, A. Aboukais, J.-F. Lamonier, I. N. Filimonov, *Appl. Catal.*, 2003, **245**, 209.
15. M. V. Tsodikov, V. V. Teplyakov, M. I. Magsumov, E. I. Shkol´nikov, E. V. Sidorova, V. V. Volkov, F. Kaptein, L. Gora, L. I. Trusov, V. I. Uvarov, *Kinet. Katal.*, 2006, **47**, 29 [*Kinet. Catal.* (*Engl. Transl.*), 2006, **47**].
16. N. Kakuta, S. Ikawa, T. Eguchi, K. Murakami, H. Ohkita, T. Mizushima, *J. Alloys Comp.*, 2006, **408**—**412**, 1078.
17. C. Amorim, M. A. Keane, *J. Chem. Technol. Biotechnol.*, 2008, **83**, 662.
18. M. E. Posin, *Techol. Mineral Salts*, 1974, **4**, Part 2.
19. H. Karaca, J. Hong, P. Fongarland, P. Roussel, A. Griboval-Constant, M. Lacroix, K. Hortmann, O. V. Safonova, A. Y. Khodakov, *Chem. Commun.*, 2010, **46**, 788.
20. N. Norman, A. Earnshaw, *Chemistry of the Elements*, 2nd ed., Pergamon, Oxford—Greenwood, 1997, 1118.
21. I. M. Kurchatov, N. I. Laguntsov, M. V. Tsodikov, A. S. Fedotov, I. I. Moiseev, *Kinet. Katal.*, 2008, 121 [*Kinet. Catal.* (*Engl. Transl.*), 2008].

Received April 20, 2011;
in revised form July 19, 2011